HHS Public Access

Author manuscript

Nat Immunol. Author manuscript; available in PMC 2009 October 01.

Published in final edited form as:

Nat Immunol. 2009 April ; 10(4): 394–402. doi:10.1038/ni.1707.

Blood-derived inflammatory dendritic cells in lymph nodes stimulate acute T_H1 immune responses

Hideki Nakano[1,2,4,6], **Kaifeng Lisa Lin**[2,6], **Manabu Yanagita**[1,5], **Chantal Charbonneau**[1], **Donald N. Cook**[4], **Terutaka Kakiuchi**[3], and **Michael D. Gunn**[1,2]

[1]Division of Cardiology, Department of Medicine, Duke University Medical Center, Durham, North Carolina 27710

[2]Department Immunology, Duke University Medical Center, Durham, North Carolina 27710

[3]Department of Immunology, Toho University School of Medicine, Tokyo 143-8540, Japan

[4]Laboratory of Respiratory Biology, National Institute of Environmental Health Sciences, National Institutes of Health, Research Triangle Park, NC 27709

Abstract

T_H1-polarized immune responses, which confer protection against intracellular pathogens, are thought to be initiated by dendritic cells (DCs) that enter lymph nodes from peripheral tissues. We found following viral infection or immunization, inflammatory monocytes were recruited into lymph nodes directly from the blood to become $CD11c^+CD11b^{hi}Gr\text{-}1^+$ inflammatory DCs, which produced abundant interleukin 12(p70) and potently stimulated T_H1 responses. This monocyte extravasation required CCR2 but not CCL2 or CCR7. Thus, inflammatory DC accumulation and T_H1 responses were markedly reduced in *Ccr2*$^{-/-}$mice, preserved in *Ccl2*$^{-/-}$ mice, and relatively increased in CCL19-CCL21-Ser-deficient *plt* mutant mice, in which all other lymph node DC types were reduced. We conclude that blood-derived inflammatory DCs play a major role in the development of T_H1 immune responses.

Keywords

lymph node; chemokine; monocytes; dendritic cells

Immune responses are initiated in lymph nodes when antigen-bearing dendritic cells (DCs) stimulate the activation and polarization of T cells1,2. In the classic view, T cell activation is stimulated primarily by migratory DC populations, such as Langerhans cells, that enter lymph nodes from the periphery via lymphatics, and most DC subtypes behave like Langerhans cells1,2. This view has changed in recent years with the findings that some

Correspondence should be addressed to M.D.G. (michael.gunn@duke.edu), Michael D. Gunn, Duke University Medical Center, Box 3547, Durham, North Carolina 27710. Tel: 919-684-0840 Fax: 919-684-8591.

[5]Present address: Department of Periodontology, Division of Oral Biology and Disease Control, Osaka University Graduate School of Dentistry, 1-8 Yamadaoka, Suita, Osaka 565-0871, Japan.

[6]These authors contributed equally to this paper.

lymph node DC subtypes arise from precursors recruited directly from the blood or only during inflammation and that, in many cases, migratory DC types do not directly activate T cells *in vivo*3–5. These findings have raised questions about which lymph node DC subtypes actually stimulate T cell activation and polarization after various immunogenic stimuli.

T_H1-polarized T cells produce interferon-γ (IFN-γ) and provide protection against viruses and other intracellular pathogens. T_H1 T cell polarization is stimulated most strongly by interleukin 12 (IL-12), which is produced by monocytes, macrophages, and certain DC subtypes upon activation6. Bioactive IL-12, IL-12(p70), is composed of two subunits: IL-12(p40), which is produced in fairly high amounts and is shared with IL-23, and IL-12(p35), whose production is more tightly regulated and represents the rate-limiting step in IL-12(p70) formation7. Among DC subtypes obtained from resting lymphoid organs, resident $CD8^+$ DCs have the greatest T_H1-polarizing activity8,9. However, this may not be true during infection or inflammation. During chronic cutaneous leishmania infection, peripheral 'inflammatory' DCs (derived from inflammatory $Gr\text{-}1^+$ monocytes that enter peripheral tissues, become DCs, and migrate to lymph nodes via lymphatics) accumulate in large numbers and display robust T_H1-polarizing activity10,11. Consistent with the idea that monocyte-derived DCs (moDCs) stimulate T_H1 responses, these responses are markedly impaired in mice lacking the chemokine receptor that mediates inflammatory monocyte migration, CCR 2 http://www.signaling-gateway.org/molecule/query?afcsid=A000625 (refs. 12–14). This abnormality has been proposed to be due to a defect in the trafficking of monocytes to sites of immunization or infection13. However, this view is not consistent with the finding that mice lacking the major CCR2 ligand, CCL2 (also known as monocyte chemoattractant protein 1, MCP-1, http://www.signaling-gateway.org/molecule/query?afcsid=A001484), have normal or increased T_H1 responses15,16. The cause of the divergent T cell responses in *Ccr2*$^{-/-}$ and *Ccl2*$^{-/-}$ mice has not been determined17.

Inflammatory DCs in lymph nodes can arise from moDCs recruited via lymphatics (peripheral moDCs) and from inflammatory monocytes that enter lymph nodes directly from the blood (blood-derived inflammatory DCs)10,11,18,19. Although inflammatory monocytes have been demonstrated to extravasate across high endothelial venules (HEVs) into lymph nodes and develop into DCs, the role that blood-derived inflammatory DCs may play in antigen-specific T cell responses has not been determined18. Here, we identify a population of $CD11c^+CD11b^{hi}Gr\text{-}1^+$ inflammatory DCs that was the major source of both IL-12(p70) production and T cell IFN-γ stimulatory activity in lymph nodes after immunization or viral infection. These inflammatory DCs arose from monocytes that entered inflamed lymph nodes directly from the blood and their accumulation in lymph nodes required CCR2, but not CCL2 or CCR7 http://www.signaling-gateway.org/molecule/query?afcsid=A000630. Inflammatory DCs were the only DC type to accumulate in the lymph nodes of mice with the paucity of lymph node T cell (*plt*) mutation, a deletion of the CCR7 ligand genes *Ccl19* and *Ccl21*-Ser, which results in a loss of all CCL19 expression and CCL21 expression in secondary lymphoid organs20, leading to increased T_H1 responses in these mice after immunization. Absence of inflammatory DC accumulation accounted for the markedly decreased T_H1 responses seen in CCR2-deficient, but not CCL2-deficient, mice.

Results

Increased T cell responses in lymph nodes of *plt* mice

We identified lymph node moDCs in the course of examining immune response abnormalities in *plt* mice. *Plt* mice display a >95% reduction in the migration of naive T cells into lymph nodes and a 50–60% decrease in total lymph node DCs21,22. However, despite these defects, *plt* mice display increased antigen-specific T cell numbers and increased antigen-specific T cell proliferation for at least 16 months after immunization23,24. On both BALB/c (Fig. 1a) and C57BL/6 (Fig. 1b) genetic backgrounds, *plt* mice displayed delayed-type hypersensitivity (DTH) responses that are about 2-fold greater than seen in wild-type mice. This increased response was independent of whether Complete Freund's adjuvant (CFA), monophosphoryl lipid A-trehalose dicorynomycolate (RIBI), or lipopolysaccharide (LPS) was used as the adjuvant for sensitization and of the number of sensitizing immunizations (Fig. 1c and data not shown). *Plt* mice also displayed contact hypersensitivity (CHS) responses that were markedly increased by day 7 and were maintained without reduction for at least eight weeks (Fig. 1d). After immunization with ovalbumin (OVA) in CFA, *plt* mice displayed a 6-fold increase in the proportion of $CD4^+$ T cells that produced IFN-γ (Fig. 1e, f), indicating the development of markedly increased T_H1 T cell responses. These increased T cell responses were not due to an intrinsic defect in T cells or DCs. After reciprocal bone marrow transplantations between wild-type and *plt* mice, the *plt* phenotype of increased DTH responses was seen in *plt* recipients, irrespective of the bone marrow donor genotype (Fig. 1g). In our hands, bone marrow transplantation typically leads to some reduction in DTH response relative to non-transplanted mice (data not shown). Like *plt* mice, CCR7-deficient mice display severe defects in the accumulation of T cells and DCs in draining lymph nodes25, but display increased T cell responses in contact hypersensitivity assays26. The cause of the paradoxically increased T cell responses seen in *plt* and CCR7-deficient mice has not been previously determined.

At baseline, T cells in *plt* lymph nodes are markedly reduced in number and are predominantly of memory phenotype, but display no obvious abnormalities in response to antigen stimulation21,23. The frequency of $CD25^+$ T regulatory cells among total T cells in *plt* lymph nodes was normal at baseline and after immunization (data not shown). Thus, T cells in *plt* mice appear to be normal. In contrast, total $CD11c^+$ DCs in the lymph nodes of naive *plt* mice displayed an increased capacity to stimulate the proliferation of allogeneic naive $CD4^+$ T cells (Fig. 1h). Nine days after immunization, a time when T cell proliferative responses in *plt* mice are increased23, total lymph node DCs from *plt* mice, bearing only the antigen administered 9 days earlier, stimulated the robust proliferation of cells from an OVA-primed DO11.10 $CD4^+$ T cell line, while DCs obtained from wild-type lymph nodes displayed no such ability (Fig. 1i). This increased ability to stimulate OVA-experienced T cells persisted for at least 28 days after immunization (Fig. 1j). These results suggest that the increased and prolonged T cell responses seen in *plt* mice are due, at least in part, to an increased and prolonged activity among lymph node DCs.

Alterations in DC subset composition in *plt* lymph nodes

To determine if the increased activity of total lymph node DCs in *plt* mice was due to alterations in the frequency of individual lymph node DC subtypes, we used the gating protocol shown in Fig. 2a to examine the frequency of six individual DC subtypes in *plt* popliteal lymph nodes at baseline and after footpad immunization. Five of these DC subtypes correspond to well-described lymph node DC populations27. These include $CD11b^{-}B220^{+}$ plasmacytoid DCs (pDCs); $CD11c^{hi}CD40^{int}$ cells (gate I), which include $CD11b^{+}CD8^{-}$DCs and $CD11b^{int}CD8^{+}$ ($CD8^{+}$) DCs; $CD11c^{int}CD40^{hi}$ dermal-derived DCs (gate II); and $CD11c^{hi}CD40^{hi}$ Langerhans cells (gate III). We also found a $CD11c^{int}CD11b^{hi}CD40^{int}$ DC population (gate IV) that displayed the phenotype described for moDCs11,28–30. These $CD11c^{int}CD40^{int}$ cells were $CD11b^{hi}$, $CD80^{+}$, $CD86^{+}$, major histocompatibility complex (MHC) class II^{+}, $CD4^{+}$, $CD8^{-}$and expressed no CCR7 (Fig. 2a and Supplementary Fig. 1 online). Such cells were present in small numbers in resting wild-type lymph nodes but were difficult to discern among other cell types. The $CD11c^{int}CD40^{int}$ cells were ablated in immunized CD11c-diphtheria toxin receptor transgenic mice after diphtheria toxin treatment, confirming their classification as DCs (data not shown).

Resting lymph nodes in *plt* mice displayed a 45% decrease in total $CD11c^{+}$ cells, but this decrease was not uniform among DC subtypes (Fig. 2b,c). Numbers of $CD11c^{int}CD40^{int}$ DCs were normal in resting *plt* lymph nodes while the absolute number of all other DC subtypes was markedly (55%–81%) reduced (Fig. 2b,d). Following subcutaneous immunization with OVA in CFA, numbers of $CD11c^{int}CD40^{int}$ DCs in *plt* lymph nodes increased normally, while all other DC subtypes displayed almost no change in number over the 8 days following immunization (Fig. 2d). By day 8, all DC subtypes in *plt* mice other than $CD11c^{int}$ $CD11b^{hi}$ $CD40^{int}$ DCs were reduced by at least 75% relative to wild-type mice (Fig. 2b,c), resulting in a markedly increased ratio of $CD11c^{int}CD11b^{hi}CD40^{int}$ DC to other DC subtypes (1:5 in wild-type vs. 2:1 in *plt*). Like *plt* mice, $Ccr7^{-/-}$ mice displayed normal numbers of $CD11c^{int}CD11b^{hi}CD40^{int}$ DCs eight days after immunization, but marked reductions in all other DC subtypes (Fig. 2d, open triangles). $Ccr7^{-/-}$ mice displayed a greater reduction in migratory DC types (gates II and III) than *plt* mice, consistent with their more complete loss of lymphatic CCR7 activity. These findings are consistent with prior studies31.

Because moDCs express the glycosyl phosphatidylinositol-anchored monocyte differentiation antigen Ly-6C for several days after their differentiation from inflammatory monocytes, they can be identified by staining with anti-Gr-1, which recognizes Ly-6C and Ly-6G30. We identified $Gr\text{-}1^{+}$ DCs in lymph nodes as a subset of $CD11c^{int}CD11b^{hi}CD40^{int}$ (region IV) DCs. Gr-1 proved to be more specific than CD40 in identifying moDCs as a distinct population and was therefore used in all subsequent experiments. In wild-type mice, $CD11b^{hi}Gr\text{-}1^{+}$ DC were rare in lymph nodes at baseline but accumulated after immunization (Fig. 3a). In *plt* mice, $CD11b^{hi}Gr\text{-}1^{+}$ DCs were abundant in lymph nodes at baseline and were markedly increased as a proportion of total lymph node DCs after immunization (Fig. 3a). The absolute number $CD11b^{hi}Gr\text{-}1^{+}$ DCs in lymph nodes was normal in *plt* mice at baseline and after immunization (Fig. 3b). $CD11b^{hi}Gr\text{-}1^{+}$ DCs in *plt* lymph nodes were $CD40^{int}$, $CD80^{+}$, $CD86^{+}$, and MHC class II^{+} (Supplementary Fig. 2 online). To ensure that

the rapid accumulation of CD11b^{hi}Gr-1^{+} DCs in lymph nodes was not a specific response to CFA immunization, we examined another model of inflammation, acute viral infection. Five days after influenza virus infection, the frequency of CD11b^{hi}Gr-1^{+} DCs increased 7-fold in the mediastinal lymph nodes of wild-type mice (Fig. 3c). In *plt* mice, the frequency of CD11b^{hi}Gr-1^{+} DCs was increased at baseline and markedly increased after viral infection (Fig. 3c). The absolute number of CD11b^{hi}Gr-1^{+} DCs in *plt* mediastinal lymph nodes was similar to that seen in wild-type mice after viral infection (Fig. 3d).

Because DC migration through lymphatics requires CCR7 activity32, the preserved CD11b^{hi}Gr-1^{+} DC accumulation in *plt* and *Ccr7*$^{-/-}$ mice suggests that these cells enter lymph nodes directly from the blood as inflammatory monocytes. To determine whether DCs were capable of entering inflamed *plt* lymph nodes via lymphatics, we injected bone marrow-derived DCs into the footpads of wild-type and *plt* mice. Injected DCs accumulated in the draining popliteal lymph nodes of wild-type mice but not *plt* mice (Fig. 3e), a finding consistent with previous reports10. In contrast, intravenous injection of bone marrow monocytes resulted in a roughly equal accumulation of donor CD11c^{+}CD11b^{hi}CD86^{+} DCs in the lymph nodes of wild-type and *plt* mice after 3 days (Fig. 3f). These results suggest that the inflammatory DCs in *plt* lymph nodes are blood-derived and do not enter lymph nodes via lymphatics.

T_H1 stimulatory activity of inflammatory DCs

The finding that CD11b^{hi}Gr-1^{+} DCs were increased in relative frequency in *plt* mice suggests that these cells may stimulate T_H1 polarization. To test this notion, we purified CD11b^{hi}Gr-1^{+} and CD8^{+} DCs from the mediastinal lymph nodes of influenza-infected C57BL/6 mice and used these cells to stimulate OVA-specific OT2 T cells *in vitro*. CD8^{+} DCs were chosen for comparison because they have been previously described as the most potent T_H1-stimulatory DC subtype8,9. CD11b^{hi}Gr-1^{+} DCs induced strikingly high amounts of T cell-generated IFN-γ relative to both CD8^{+} DCs purified from the same lymph nodes and total DCs purified from the spleens of naive mice (Fig. 4a). This difference in IFN-γ production was not due to differences in overall T cell proliferation (Fig. 4b) or T cell survival (data not shown). To determine why lymph node CD11b^{hi}Gr-1^{+} DCs had such potent IFN-γ stimulatory activity, we examined the production of IL-12 by lymph node DC subtypes. Individual mediastinal lymph node DC subtypes were purified by flow cytometry 4 days after influenza infection and stimulated *in vitro* with LPS and anti-CD40. Under these conditions, CD11b^{hi}Gr-1^{+} DCs, CD8^{+} DCs, and naive splenic DCs all produced significant amounts of the IL-12 subunit, p40 (Fig. 4c). However, only CD11b^{hi}Gr-1^{+} DCs produce detectable amounts of complete IL-12(p70) (Fig. 4d).

To determine the extent to which CD11b^{hi}Gr-1^{+} DC actually captured antigen *in vivo*, we immunized mice subcutaneously with OVA conjugated to Alexafluor-647 (AF-647) in CFA and examined the percentage of each DC subtype in lymph nodes that were AF-647^{+}. Surprisingly, 3 days post immunization, the percentage of CD11b^{hi}Gr-1^{+} DCs that contained labeled antigen was much higher than any other lymph node DC subtype (Fig. 4e,f). In addition, CD11b^{hi}Gr-1^{+} DCs appeared to capture more antigen on a per cell basis than other lymph node DC types, based on the fluorescent intensity of AF-647^{+} cells (Fig. 4e). AF-647

staining was not detected on either monocytes or DCs in the blood of immunized mice (Fig. 4g), suggesting that antigen capture by CD11b^{hi}Gr-1^{+} DC occurred within the lymph node.

moDC accumulation requires CCR2 but not CCL2

Based on the above findings, we concluded that monocytes enter inflamed lymph nodes directly from the blood, that they give rise to inflammatory DCs with potent T_H1 stimulatory activity, and that the entry of these cells into lymph node was CCR7-independent. Because inflammatory monocyte migration is typically CCR2-dependent, we recognized that, if correct, this model would provide an explanation for the reduced T_H1 responses seen in *Ccr2*$^{-/-}$ mice. We therefore examined the accumulation of inflammatory DCs in the lymph nodes of CFA-immunized and influenza-infected mice. Consistent with our hypothesis, CD11b^{hi}Gr-1^{+} DCs were markedly reduced in the draining lymph nodes of immunized *Ccr2*$^{-/-}$ mice (Fig. 5a). CD11b^{hi}Gr-1^{+} DC accumulation was also markedly reduced in the mediastinal lymph nodes of *Ccr2*$^{-/-}$ mice during influenza infection (Fig. 5b,d). Importantly, when *Ccl2*$^{-/-}$ mice were examined in the same manner, they displayed no reduction in CD11b^{hi}Gr-1^{+} DC accumulation (Fig. 5c,d). This finding demonstrates that the accumulation of CD11b^{hi}Gr-1^{+} DCs in lymph nodes requires CCR2 but not CCL2. In contrast, the accumulation of DCs in footpads appears to be CCL2-dependent. The number of CD11c^{+}CD11b^{+} DCs found in footpads 3 days after CFA injection was reduced to a similar extent in *Ccr2*$^{-/-}$ and *Ccl2*$^{-/-}$ mice (Fig. 5e).

To confirm that the difference in inflammatory DC accumulation seen in *Ccr2*$^{-/-}$ and *Ccl2*$^{-/-}$ mice was due to a difference in inflammatory monocyte trafficking, we examined the accumulation of bone marrow monocytes in lymph nodes two hours after IV injection. To stimulate inflammation, mice were injected in the hind footpad with OVA plus CFA and, 72 hours later, injected by tail vein with labeled Gr-1^{+} bone marrow monocytes. When injected into wild-type mice, the migration of *Ccr2*$^{-/-}$ monocytes to the draining popliteal lymph nodes was significantly reduced relative to wild-type monocytes (Fig. 5f). In contrast, monocyte migration to lymph nodes in *Ccl2*$^{-/-}$ mice was not decreased relative to wild-type mice (Fig. 5f). In these studies, monocyte migration to the inflamed footpads was reduced to a similar extent in *Ccr2*$^{-/-}$ and *Ccl2*$^{-/-}$ mice (Fig. 5g).

To determine why monocyte extravasation into lymph nodes does not require CCL2, we examined the concentrations of various CCR2 ligand proteins in resting and inflamed lymph nodes and footpads. After CFA injection into footpads, CCL2 was abundantly produced in the footpad, with CCL8 (also known as MCP-2) seen at much lower concentrations and no CCL7 (MCP-3) or CCL12 (MCP-5) detected (Fig. 5h). At the same time, the draining popliteal lymph nodes contained high concentrations of both CCL2 and CCL8 (Fig. 5i). In contrast, CCL8 was the predominant CCR2 ligand expressed in mediastinal lymph nodes during influenza infection, with little CCL2 detected (Fig. 5j). These results provide a mechanistic basis for our finding that inflammatory monocyte extravasation was CCL2-dependent in inflamed footpads but CCL2-independent in inflamed lymph nodes and account for the divergence in inflammatory DC accumulation seen in the lymph nodes of *Ccr2*$^{-/-}$ and *Ccl2*$^{-/-}$ mice.

Reduced T_H1 stimulatory DCs in *Ccr2*$^{-/-}$ lymph nodes

The finding that blood-derived inflammatory DCs accumulated in the lymph nodes of *Ccl2*$^{-/-}$ but not *Ccr2*$^{-/-}$ mice strongly suggests that these cells play an important role in stimulating T_H1 immune responses. To directly compare T_H1 T cell polarization in *Ccr2*$^{-/-}$ and *Ccl2*$^{-/-}$ mice, we examined lymph node T cells after subcutaneous immunization with OVA in CFA. Upon restimulation with OVA, IFN-γ production by T cells from *Ccr2*$^{-/-}$ mice was markedly reduced while T cells from *Ccl2*$^{-/-}$ mice displayed increased IFN-γ production (Fig. 6a). At the same time, T cells from *Ccr2*$^{-/-}$ and *Ccl2*$^{-/-}$ mice produced normal amounts of IL-2 (Fig. 6b). To confirm that the reduced T cell IFN-γ production seen in *Ccr2*$^{-/-}$ mice was due to a reduction in DC T_H1-stimulatory activity, we examined this activity in wild-type and *Ccr2*$^{-/-}$ lymph node DC populations. To obtain sufficient cell numbers, DCs were purified from the mediastinal lymph nodes of influenza-infected mice. As above, CD11b^{hi}Gr-1^{+} DCs purified from wild-type lymph nodes stimulated robust T cell IFN-γ production (Fig. 6c). CD11b^{hi}Gr-1^{+} DCs were not present in the lymph nodes, spleens, or blood of infected *Ccr2*$^{-/-}$ mice and therefore could not be tested. CD11b^{hi}Gr-1^{-} DCs purified from wild-type lymph nodes stimulated low amounts of IFN-γ, demonstrating a potency of about 25% that of Gr-1^{+} DCs. Among CD11b^{hi}Gr-1^{-} DCs purified from *Ccr2*$^{-/-}$ lymph nodes, this activity was reduced, suggesting that a portion of inflammatory DCs may display a Gr-1^{-} phenotype due to loss of Ly6-C expression30. CD8^{+} DCs from *Ccr2*$^{-/-}$ mice also stimulated production of low amounts of IFN-γ, with an activity similar to wild-type CD8^{+} DCs (compare Figs. 6c and 4a) but much lower than CD11b^{hi} Gr-1^{+} DCs. These differences in T_H1-stimulating activity are not due to differences in the stimulation of T cell proliferation (Fig. 6d). We conclude that the reduction in T_H1 responses seen in *Ccr2*$^{-/-}$ mice was due to an absence of T_H1-stimulatory inflammatory DC within inflamed lymph nodes.

Discussion

Current evidence suggests that multiple DC subtypes cooperate to stimulate T cell responses. Resident lymph node DCs present antigen that drains to lymph nodes and stimulate the initial steps of T cell activation, including increased CD69 expression and retention within lymph nodes33,34. Migratory DCs transport high amounts of antigen to lymph nodes and stimulate the next steps of T cell activation, namely IL-2 production and proliferation33,34. Both these DC activities are required to stimulate robust T cell proliferation and the generation of effector responses33,34. As immune stimulation continues, monocytes recruited to peripheral sites develop into inflammatory DCs, which migrate to lymph nodes to provide a continuing stimulus for T cell proliferation or polarization11.

Here, we demonstrate that an additional lymph node DC type, blood-derived inflammatory DCs, plays a key role in the development of acute T cell responses, primarily by stimulating T cell polarization. Blood-derived inflammatory DCs appear in lymph nodes as CD11c^{+}CD40^{int}CD11b^{hi}Gr-1^{+} cells that accumulate early after a T_H1-polarizing stimulus, capture antigen, produce large amounts of IL-12(p70), and stimulate CD4^{+} T cell IFN-γ production much more potently than other lymph node DC subtypes. Our findings indicate

that CD11c^{+}CD40^{int}CD11b^{hi}Gr-1^{+} DCs arise from monocytes that enter lymph nodes directly from the blood. The accumulation of inflammatory DCs in lymph nodes requires CCR2, but not CCL2 or CCR7 and therefore provides an explanation for the defects in T cell polarization seen in *Ccr2*$^{-/-}$, *Ccl2*$^{-/-}$ and *plt* mice. These defects have been recognized for some time, but have been difficult to reconcile with the classic view of T cell activation strictly by lymphatic-born DCs17.

Our findings strongly suggest that both CCL2 and CCL8 can stimulate monocyte extravasation into lymph nodes. Consistent with the relative concentrations of these chemokines, we find that monocyte extravasation is completely CCL2-independent in mediastinal lymph nodes and somewhat CCL2 dependent in popliteal lymph nodes (data not shown). A previous study demonstrated that monocyte extravasation into lymph nodes can be CCL2-dependent19. As reported in that paper, we find little CCL2 mRNA in inflamed lymph nodes (data not shown). Because most CCL2 protein in lymph nodes is produced remotely, lymph node CCL2 concentrations and the contribution of CCL2 to lymph node monocyte extravasation are likely to depend on the specific inflammatory stimulus, the time after stimulation, and the peripheral tissue being drained. Direct proof that CCL8 stimulates monocyte extravasation into lymph nodes will probably require an examination of mice that lack this chemokine.

We find that CCL2 is the predominant CCR2 ligand expressed in inflamed footpads and that inflammatory monocyte migration to footpads is CCL2-dependent. For this reason, *Ccr2*$^{-/-}$ and *Ccl2*$^{-/-}$ mice display similar defects in the accumulation of DCs in footpads and, presumably, similar alterations in lymph node DC populations derived from peripheral tissues. Thus, the presence of blood-derived inflammatory DCs appears to be the only substantial difference in lymph node DC populations between *Ccr2*$^{-/-}$ and *Ccl2*$^{-/-}$ mice. This difference is closely associated with the ability to develop T_H1 responses, demonstrating that blood-derived inflammatory DCs provide a T cell polarizing activity that is sufficient for robust T_H1 immune response. Blood-derived inflammatory DCs are likely to also be necessary for such responses under the conditions we examined, as no other lymph node DC subtype displays a comparable T_H1-stimulatory activity. However, it is possible that both *Ccr2*$^{-/-}$ and *Ccl2*$^{-/-}$ mice lack a peripheral DC type that would be sufficient to stimulate T_H1 polarization in the absence of blood-derived inflammatory DCs. T cell proliferative responses are normal in *Ccr2*$^{-/-}$ mice, demonstrating that blood-derived inflammatory DCs are not necessary for T cell proliferation35.

The immune response abnormalities seen in *plt* mice involve defects in both T cell polarization and the contraction phase of T cell response. *Plt* lymph nodes contain normal numbers of blood-derived inflammatory DCs, but are markedly deficient in all other, CCR7-dependent DC types. The increased T_H1 responses seen in *plt* mice provide additional evidence that blood-derived inflammatory DCs are sufficient for T_H1 polarization, but also suggest that this response is normally modulated by one or more CCR7-dependent DC types. *Plt* mice display normal T cell proliferative responses, suggesting that blood-derived inflammatory DCs can provide a stimulatory activity that is sufficient to drive T cell proliferation. This conclusion is supported by our finding that lymph node CD11b^{+}Gr-1^{+} DCs stimulated T cell proliferation *in vitro* to an extent comparable to other lymph node DC

types. *Plt* mice also display a marked prolongation of T cell responses, increased antigen-specific T cell numbers, and a significant decrease in the percentage of antigen-specific lymph node T cells that undergo apoptosis after immunization23,24. These findings suggest that a CCR7-dependent DC population stimulates the contraction phase of T cell responses, perhaps by inducing the apoptosis of activated T cells36.

Our findings suggest that inflammatory DCs capture antigen within lymph nodes, as we detected no antigen on circulating monocytes. This may occur via the capture of antigen in free form within lymph nodes or via the transfer from other DCs5,37. Based on the differing responses of *plt* and *Ccr7*$^{-/-}$ mice, we speculate that inflammatory DCs obtain antigen via the transfer from other DC types. *Plt* mice express low amounts of CCL21 on lymphatics and display some migration of Langerhans and dermal DCs to lymph nodes20,22. In contrast, *Ccr7*$^{-/-}$ mice lack all CCR7 activity and display almost no detectable migration of these cell types25. Because *plt* and *Ccr7*$^{-/-}$ mice would be expected to have normal amounts of free antigen in lymph nodes, any differences in antigen trafficking to lymph nodes are likely to be due to transport by migratory DCs. The activity of *Ccr7*$^{-/-}$ migratory DCs is not sufficient to support CD4^{+} T cell proliferation after OVA-CFA immunization34. Similarly, during influenza infection, antigen transport in *Ccr7*$^{-/-}$ mice is insufficient to support CD8^{+} T cell proliferation and results in only limited CD4^{+} T cell responses38. Consistent with our findings, those limited CD4^{+} T cell responses include a marked increase in T cell IFN-γ production38. The amount of antigen in lymph nodes required to stimulate T cell activation is very low but displays a sharp threshold that can be achieved with very few DCs39. It appears that this threshold is reached in *plt* mice, but in some cases, not *Ccr7*$^{-/-}$ mice. The increased T cell responses in *plt* mice appear to be due to their increased proportion of blood-derived inflammatory DCs, suggesting that differences in immune response between *plt* and *Ccr7*$^{-/-}$ mice are due to the delivery of antigen to these cells by migratory DC types.

Under the conditions we examined, blood-derived inflammatory DCs have a potent T_H1-stimulatory activity, probably due to their robust production of IL-12(p70). CD11b^{+} Gr-1^{+} DCs obtained from IL-12(p35)-deficient mice fail to stimulate T cell IFN-γ production *in vitro* (data not shown). These cells may also stimulate T_H2 T cell polarization. Inflammatory DCs stimulate T_H2 responses after intraperitoneal injection of OVA in alum adjuvant40. Two publications41,42 and our own unpublished findings demonstrate that *plt* mice display increased T_H2 responses when given a T_H2-polarizing stimulus. At present, it is not clear whether increased T_H2 responses in *plt* mice are due to an increased T_H2 polarizing activity or to a decreased ability to modulate immune responses. T_H2 responses are not decreased in *Ccr2*$^{-/-}$ mice, demonstrating that blood-derived inflammatory DCs are not necessary for T_H2 polarization. Delineating the specific role that blood-derived inflammatory DCs play, relative to other DC types, in regulating immune responses will have important implications for efforts to enhance or inhibit these responses in clinical settings.

Methods

Mice

BALB/c, C3H/He, and C57BL/6 mice were purchased from Charles River Labs. CD11c-DTR, CD45.1, DO11.10, OT2, *Ccr2*$^{-/-}$ and *Ccl2*$^{-/-}$ mice were purchased from The Jackson

Laboratory. DDD/1-*plt* mice were backcrossed to BALB/c mice 10 times and to C57BL/6 mice 11 times23, and maintained at Duke University Medical Center and Toho University School of Medicine. All mice were kept under specific pathogen-free conditions and used at 7 to 15 wk of age. Mice were immunized subcutaneously at two sites on the back with 100 μg chicken OVA (Sigma-Aldrich) in RIBI adjuvant (Sigma-Aldrich) or in a 1:1 emulsion of PBS and CFA (Difco or Sigma-Aldrich) or in the footpad with 10–20 μg OVA in CFA. For influenza infections, mice were anesthetized with ketamine-xylazine (100 mg/kg-10mg/kg) i.p., then infected with H1N1 influenza virus strain A/Puerto Rico/8/34 (PR8) (ATCC, Manassas, VA, VR-95) intranasally (30 μl of 5×10^5 $TCID_{50}$/ml virus per mouse). Body weight of infected mice was monitored daily. All experiments were carried out according to institutional guidelines and approved by the Duke IACUC committee.

Antibodies

Purified, biotinylated or Alexa Fluor 488, Allophycocyanine (APC), FITC, Phycoerythrin (PE), PE-Cy5, PE-Cy5.5, APC-Cy7, APC-AF750, PE-Cy7 or PE-Texas Red-conjugated mAbs specific for the following mouse antigens were used; CD3 (145-2C11), CD4 (RM4-5), CD8α (53-6.7), CD11b (M1/70), CD11c (HL3), CD16/32 (2.4G2), CD19 (1D3), CD40 (3/23), CD44 (IM7), CD45R/B220 (RA3-6B2), CD49b (DX5), CD62L (MEL-14), CD80 (16-10A1), CD86 (GL1), I-A^b (25-9-17), I-A^d (AMS-32-1), I-A/I-E (2G9), Ly6C/G (Gr-1, RB6-8C5), Ly6G (1A8), Ly76 (TER119), DO11.10 TCR clonotype (KJ1-26), Sca-1 (E13-161.7), c-kit (2B8), CCR3 (83101), CCR7 (4B12) (purchased from BD Pharmingen, BioLegend, CALTAG or eBioscience). The following isotype control mAbs were used; mouse IgG_1 (G155-178), rat IgG_1 (R3-34), rat IgG_{2a} (R35-95), rat IgG_{2b} (A95-1), hamster IgG (G235-2356) (BD Pharmingen or eBioscience).

Flow cytometric analysis

Cells were stained with antibodies in Mg^{2+}- and Ca^{2+}-free Dulbecco's PBS (Invitrogen) containing 3% FCS, 5% normal mouse serum, 5% normal rat serum, 5 μg/ml anti-CD16/32 mAbs and 10 mM EDTA for 30 min at 0°C. For cell sorting, HBSS was used instead of Dulbecco's PBS. After washing, stained cells were analyzed on a FACS Calibur™ or FACS LSRII™ flow cytometer (Becton Dickinson) and CELLQuest™ or FACS Diva™ software, respectively. $CD3^+$ T cells, $CD19^+$ B cells, 7-aminoactinomycin D^+ (7-AAD; BD Pharmingen) dead cells and $FL3^+$ autofluorescent cells were excluded from data for lymph node DC analysis.

DC isolation and sorting

DCs were prepared as previously described with some modifications43. Lymph nodes or spleens were minced in Mg^{2+}- and Ca^{2+}-free HBSS (Invitrogen) containing 5% FCS and 10 mM HEPES pH 7.4 (GIBCO), then digested with 1 mg/ml of collagenase A (Roche) and 0.2 mg/ml of DNase I (Sigma-Aldrich) for 35 min at 37°C. EDTA (20 mM final concentration) was added for 5 min at 25°C. Single cell suspensions were prepared using a 70 μm-CellStrainer™ (Falcon) nylon mesh, layered over RPMI 1640 containing 10% FCS and 16% Metrizamide (Accurate Chemical and Scientific), or 17.2% Nycodenz (Accurate Chemical and Scientific), and centrifuged at 450*g* for 20 min at 25°C. Low-density cells at the

interface were collected and washed with HBSS containing 5 % FCS, 10 mM HEPES pH 7.4 plus 10 mM EDTA.

To purify total $CD11c^+$ DCs, low density cells from lymph nodes were incubated with biotinylated anti-CD11c and streptavidin-conjugated MACS beads (Miltenyi), then positively sorted on a magnetic activated cell sorter (MACS, Miltenyi) according to the manufacture's instruction. Over 98% of the sorted cells were $CD11c^+$. To purify DC subsets, cells were sorted as described previously43. Briefly, low density lymph node cells were stained with anti-CD3, CD8a, CD11b, CD11c, CD19, Ly6C/G mAbs for 30 min at 0°. After washing twice, individual DC subsets among $CD11c^+CD3^-CD19^-$ cells were sorted on a FACS Vantage™ flow cytometer (Becton Dickinson). Cell purity after sorting was 85~95%.

T cell culture and proliferation assays

Naive $CD4^+$ T cells from DO11.10, OT2, or C3H/He mice were prepared as previously described43. Briefly, single cells suspensions of pooled lymph nodes and spleens were incubated with 1.25 μg/ml biotinylated anti-CD8, CD11b, CD11c, CD16/32, CD19, CD25, B220, CD49b, Ly6/G and TER119 for 30 min at 0°C, then streptavidin-conjugated MACS beads (Miltenyi) for 20 min at 0°C, negatively selected on a MACS LD column, and centrifuged on percoll (50% and 60%) (Invitrogen). Cells at the 50–60% percoll interface were collected as naive $CD4^+$ T cells. >97% of the purified cells were $CD4^+$, and >90% $CD45RB^+CD44^{int/lo}$. Cells were cultured in cRPMI-10 (RPMI-1640 (Invitrogen), 10% FCS (GIBCO), 20 mM HEPES pH 7.4, 2-mercaptoethanol (Sigma-Aldrich), 50 U/ml Penicillin, and 50 μg/ml Streptomycin) in U-bottom 96-well plates at 37°C in 5% CO_2. To prepare the OVA-specific T cell line, 5×10^5 naive DO11.10 $CD4^+$ T cells were cultured with 1 μM $OVA_{323–339}$ peptide and 10^6 30 Gy-irradiated splenic low density cells in 2 ml cRPMI-10 supplemented 20 U/ml IL-2 (Shionogi) in 24-well plates. The stimulated $CD4^+$ T cells were maintained in cRPMI-10 supplemented 10 U/ml IL-2 and restimulated with 1 μM $OVA_{323–339}$ plus 10^6 spleen cells every 2–3 weeks. OVA-primed $CD4^+$ T cells were rested for at least 6 days before use. For proliferation assays, 10^5 naive $CD4^+$ T cells or 5×10^4 cells from the DO11.10 T cell line were co-cultured with freshly isolated and irradiated DCs in 200 μl cRPMI-10 in U-bottom 96-well plates for 3 to 6 days and T cell proliferation measured either by pulsing with 1.25μCi $[^3H]$-thymidine (Amersham Bioscience) during the final 6 h of culture and measuring incorporation on a Matrix 96 direct beta counter (Packard Instruments) or by pulsing with 10 nM BrdU (Roche) in the final 3–6 h of culture, then measuring incorporation using a BrdU-ELISA kit (Roche) according to the manufacture's instructions.

OVA re-stimulation of total lymph node cells

Total cells were isolated from the draining lymph nodes of immunized wild-type, *plt*, *Ccr2*$^{-/-}$, or *Ccl2*$^{-/-}$ mice and cultured in the presence of 1 μg/ml OVA for 48 h. Cytokine production was measured by intracellular staining for IFN-γ and by analysis of supernatants for IL-2 and IFN-γ by ELISA. For ELISA assays, aliquots of T cell culture supernatants were collected before $[^3H]$-thymidine or BrdU labeling and assayed by Opt-EIA (BD Bioscience) according to the manufacture's instructions.

Delayed type hypersensitivity and contact hypersensitivity assays

Seven days after subcutaneous immunization with OVA-CFA or OVA-RIBI immunized and naive mice were injected intracutaneously with 10 μl PBS into right ear and 10 μl PBS with 25 μg OVA into left ear. Ear thickness was measured using a Peacock dial thickness gauge (Ozaki MFG) before and 24 h after elicitation. Ear swelling was calculated as the difference in thickness between 0 and 24 h. Reciprocal bone marrow transplants between BALB/c and BALB/c-*plt* mice were performed as previously described44. Briefly, 10^7 bone marrow cells were injected intravenously into 8.5 Gy gamma-irradiated recipients 30 days prior to immunization. For contact hypersensitivity assays, mice were sensitized with 50 μl 100 mg/ml oxazolone in vehicle (acetone:Olive oil, 4:1) on their shaved abdomens. 7 to 56 days later, their right ears were challenged with 10 μl of 10mg/ml oxazolone in vehicle and their left ears with vehicle alone. Ear thickness was measured before elicitation and at 24 h and ear swelling calculated as above.

DC migration assay

BALB/c BM-derived DCs were prepared by culturing bone marrow cells at 1×10^6/ml in cRPMI1640, 10% FBS, and 3.3 ng/ml GM-CFS (R&D), harvested at day 9, labeled with CFSE, then injected into footpads (8×10^5/pad) of anesthetized BALB/c or BALB/c-*plt* mice. Before or 1 – 3 days after DC injection, draining popliteal lymph nodes were harvested, prepared as above, and the number of $CFSE^+CD11c^+$autofluorescence$^-$ cells determined by flow cytometric analysis.

Monocyte purification, transfer, and migration

Bone marrow cells were collected in RPMI 10% FBS, prepared as single cell suspensions, and washed. Red blood cells were lysed using ACK buffer and the remaining cells incubated with 1.25 μg/ml biotinylated anti-CD3, CD4, CD8, CD11c, CD19, Sca-1, B220, c-kit, $I\text{-}A^b$, and TER119, and FITC-labeled anti-CCR3 and Ly6G for 30 min at 0°C followed by streptavidin-conjugated and anti-FITC MACS beads (Miltenyi) for 20 min at 0°C and negatively selected over a MACS LD or LS column. The resulting monocytes were labeled with CFSE and $3–6 \times 10^6$ injected intravenously into recipient mice 3 days after footpad injection of 10 μl OVA+CFA. Two hours later, the popliteal lymph nodes and footpads of recipient mice were harvested, digested with collagenase A and DNase I, processed for DC isolation as above using an 18% nycodenz gradient, and subjected to flow cytometric analysis. Donor monocytes were identified as $CFSE^+Ly6C^{hi}CD11b^+Ly6G^-$ autofluorescence$^-$ cells.

OVA antigen uptake by DC and monocytes

C57BL/6 mice were immunized on the back with OVA+CFA (Sigma) (100 μg/site) or OVA-AF647 (Invitrogen) +CFA. After 3 days, draining lymph nodes and blood cells were examined for AF647 fluorescence by flow cytometry.

CCR2 ligands expression in footpad and lymph nodes

C57BL/6 mice were immunized in the footpads with OVA+CFA (10 μg/FP), infected with influenza virus as above, or left untreated (day 0). On days 1 and 3, mice were sacrificed,

and their footpads, draining popliteal lymph nodes, or mediastinal lymph nodes harvested. Tissues were frozen and thawed once, and then homogenized by bead milling (Glen Mill) with vortexing in a FastPrep FP120 homogenizer (Thermo Savant). Supernatants were harvested by centrifugation and assayed for CCR2 ligands by ELISA. Quantikine® kits (R&D system) were used for measuring CCL2 and CCL12, Instant ELISA (Bender MedSystems) was used for CCL7. For CCL8 ELISAs, antibody pairs and recombinant proteins were purchased from R&D system and PeproTech, respectively.

Statistics

All numerical data were analyzed for significance by ANOVA or unpaired Student's *t*-test using Prism software, as indicated in the figure legends.

Supplementary Material

Refer to Web version on PubMed Central for supplementary material.

Acknowledgments

We thank K. Nakano for excellent technical assistance and J. Whitesides, P. McDermott, and L. Olive for expert cell sorting. Supported by NIH grants AI047262 and HL085473 (MDG), the Japanese Ministry of Science and Technology (1579054, HN; 14021121, TK), the Duke Human Vaccine Institute (HN), the Japan Health Sciences Foundation (KH51052, TK), the Japan Society for the Promotion of Science (10670606, 12670621, TK) and the Japan Society for the promotion of Science for Young Scientists (MY), and in part by the intramural branch of the NIEHS, NIH.

References

1. Steinman RM, Pack M, Inaba K. Dendritic cells in the T-cell areas of lymphoid organs. Immunol Rev. 1997; 156:25–37. [PubMed: 9176697]
2. Banchereau J, Steinman RM. Dendritic cells and the control of immunity. Nature. 1998; 392:245–252. [PubMed: 9521319]
3. Villadangos JA, Heath WR. Life cycle, migration and antigen presenting functions of spleen and lymph node dendritic cells: limitations of the Langerhans cells paradigm. Semin Immunol. 2005; 17:262–272. [PubMed: 15946854]
4. Shortman K, Naik SH. Steady-state and inflammatory dendritic-cell development. Nat Rev Immunol. 2007; 7:19–30. [PubMed: 17170756]
5. Allan RS, et al. Migratory dendritic cells transfer antigen to a lymph node-resident dendritic cell population for efficient CTL priming. Immunity. 2006; 25:153–162. [PubMed: 16860764]
6. Trinchieri G. Interleukin-12: a proinflammatory cytokine with immunoregulatory functions that bridge innate resistance and antigen-specific adaptive immunity. Annu Rev Immunol. 1995; 13:251–276. [PubMed: 7612223]
7. Brombacher F, Kastelein RA, Alber G. Novel IL-12 family members shed light on the orchestration of Th1 responses. Trends Immunol. 2003; 24:207–212. [PubMed: 12697453]
8. Pulendran B, et al. Distinct dendritic cell subsets differentially regulate the class of immune response in vivo. Proc Natl Acad Sci USA. 1999; 96:1036–1041. [PubMed: 9927689]
9. Maldonado-Lopez R, et al. CD8alpha+ and CD8alpha- subclasses of dendritic cells direct the development of distinct T helper cells in vivo. J Exp Med. 1999; 189:587–592. [PubMed: 9927520]
10. Qu C, et al. Role of CCR8 and other chemokine pathways in the migration of monocyte-derived dendritic cells to lymph nodes. J Exp Med. 2004; 200:1231–1241. [PubMed: 15534368]
11. Leon B, Lopez-Bravo M, Ardavin C. Monocyte-derived dendritic cells formed at the infection site control the induction of protective T helper 1 responses against Leishmania. Immunity. 2007; 26:519–531. [PubMed: 17412618]

12. Boring L, et al. Impaired monocyte migration and reduced type 1 (Th1) cytokine responses in C-C chemokine receptor 2 knockout mice. J Clin Invest. 1997; 100:2552–2561. [PubMed: 9366570]
13. Peters W, Dupuis M, Charo IF. A mechanism for the impaired IFN-gamma production in C-C chemokine receptor 2 (CCR2) knockout mice: role of CCR2 in linking the innate and adaptive immune responses. J Immunol. 2000; 165:7072–7077. [PubMed: 11120836]
14. Peters W, et al. Chemokine receptor 2 serves an early and essential role in resistance to Mycobacterium tuberculosis. Proc Natl Acad Sci USA. 2001; 98:7958–7963. [PubMed: 11438742]
15. Lu B, et al. Abnormalities in monocyte recruitment and cytokine expression in monocyte chemoattractant protein 1-deficient mice. J Exp Med. 1998; 187:601–608. [PubMed: 9463410]
16. Gu L, et al. Control of TH2 polarization by the chemokine monocyte chemoattractant protein-1. Nature. 2000; 404:407–411. [PubMed: 10746730]
17. Luther SA, Cyster JG. Chemokines as regulators of T cell differentiation. Nat Immunol. 2001; 2:102–107. [PubMed: 11175801]
18. Geissmann F, et al. Blood monocytes: distinct subsets, how they relate to dendritic cells, and their possible roles in the regulation of T-cell responses. Immunology and cell biology. 2008; 86:398–408. [PubMed: 18392044]
19. Palframan RT, et al. Inflammatory chemokine transport and presentation in HEV: a remote control mechanism for monocyte recruitment to lymph nodes in inflamed tissues. J Exp Med. 2001; 194:1361–1373. [PubMed: 11696600]
20. Nakano H, Gunn MD. Gene Duplications at the Chemokine Locus on Mouse Chromosome 4: Multiple Strain-Specific Haplotypes and the Deletion of Secondary Lymphoid-Organ Chemokine and EBI-1 Ligand Chemokine Genes in the plt Mutation. J Immunol. 2001; 166:361–369. [PubMed: 11123313]
21. Nakano H, et al. A novel mutant gene involved in T-lymphocyte-specific homing into peripheral lymphoid organs on mouse chromosome 4. Blood. 1998; 91:2886–2895. [PubMed: 9531599]
22. Gunn MD, et al. Mice lacking expression of secondary lymphoid organ chemokine have defects in lymphocyte homing and dendritic cell localization. J Exp Med. 1999; 189:451–460. [PubMed: 9927507]
23. Mori S, et al. Mice Lacking Expression of the Chemokines CCL21-Ser and CCL19 (plt mice) Demonstrate Delayed but Enhanced T cell Immune Responses. J Exp Med. 2001; 193:207–217. [PubMed: 11148224]
24. Yasuda T, et al. Chemokines CCL19 and CCL21 promote activation-induced cell death of antigen-responding T cells. Blood. 2007; 109:449–456. [PubMed: 16973962]
25. Forster R, et al. CCR7 coordinates the primary immune response by establishing functional microenvironments in secondary lymphoid organs. Cell. 1999; 99:23–33. [PubMed: 10520991]
26. Schneider MA, et al. CCR7 is required for the in vivo function of CD4+ CD25+ regulatory T cells. J Exp Med. 2007; 204:735–745. [PubMed: 17371928]
27. Ruedl C, et al. Anatomical origin of dendritic cells determines their life span in peripheral lymph nodes. J Immunol. 2000; 165:4910–4916. [PubMed: 11046016]
28. Naik SH, et al. Intrasplenic steady-state dendritic cell precursors that are distinct from monocytes. Nat Immunol. 2006; 7:663–671. [PubMed: 16680143]
29. Varol C, et al. Monocytes give rise to mucosal, but not splenic, conventional dendritic cells. J Exp Med. 2007; 204:171–180. [PubMed: 17190836]
30. Lin KL, et al. CCR2+ monocyte-derived dendritic cells and exudate macrophages produce influenza-induced pulmonary immune pathology and mortality. J Immunol. 2008; 180:2562–2572. [PubMed: 18250467]
31. Ohl L, et al. CCR7 governs skin dendritic cell migration under inflammatory and steady-state conditions. Immunity. 2004; 21:279–288. [PubMed: 15308107]
32. Randolph GJ, Angeli V, Swartz MA. Dendritic-cell trafficking to lymph nodes through lymphatic vessels. Nat Rev Immunol. 2005; 5:617–628. [PubMed: 16056255]
33. Itano AA, et al. Distinct dendritic cell populations sequentially present antigen to CD4 T cells and stimulate different aspects of cell-mediated immunity. Immunity. 2003; 19:47–57. [PubMed: 12871638]

34. Allenspach EJ, et al. Migratory and lymphoid-resident dendritic cells cooperate to efficiently prime naive CD4 T cells. Immunity. 2008; 29:795–806. [PubMed: 18951047]
35. DePaolo RW, Rollins BJ, Kuziel W, Karpus WJ. CC chemokine ligand 2 and its receptor regulate mucosal production of IL-12 and TGF-beta in high dose oral tolerance. J Immunol. 2003; 171:3560–3567. [PubMed: 14500652]
36. Legge KL, Braciale TJ. Lymph node dendritic cells control CD8+ T cell responses through regulated FasL expression. Immunity. 2005; 23:649–659. [PubMed: 16356862]
37. Sixt M, et al. The conduit system transports soluble antigens from the afferent lymph to resident dendritic cells in the T cell area of the lymph node. Immunity. 2005; 22:19–29. [PubMed: 15664156]
38. Heer AK, Harris NL, Kopf M, Marsland BJ. CD4+ and CD8+ T cells exhibit differential requirements for CCR7-mediated antigen transport during influenza infection. J Immunol. 2008; 181:6984–6994. [PubMed: 18981118]
39. Henrickson SE, et al. T cell sensing of antigen dose governs interactive behavior with dendritic cells and sets a threshold for T cell activation. Nat Immunol. 2008; 9:282–291. [PubMed: 18204450]
40. Kool M, et al. Alum adjuvant boosts adaptive immunity by inducing uric acid and activating inflammatory dendritic cells. J Exp Med. 2008; 205:869–882. [PubMed: 18362170]
41. Grinnan D, et al. Enhanced allergen-induced airway inflammation in paucity of lymph node T cell (plt) mutant mice. J Allergy Clin Immunol. 2006; 118:1234–1241. [PubMed: 17157652]
42. Xu B, et al. Lack of lymphoid chemokines CCL19 and CCL21 enhances allergic airway inflammation in mice. Int Immunol. 2007; 19:775–784. [PubMed: 17513879]
43. Nakano H, Yanagita M, Gunn MD. CD11c(+)B220(+)Gr-1(+) cells in mouse lymph nodes and spleen display characteristics of plasmacytoid dendritic cells. J Exp Med. 2001; 194:1171–1178. [PubMed: 11602645]
44. Nakano H, et al. Genetic defect in T lymphocyte-specific homing into peripheral lymph nodes. Eur J Immunol. 1997; 27:215–221. [PubMed: 9022021]

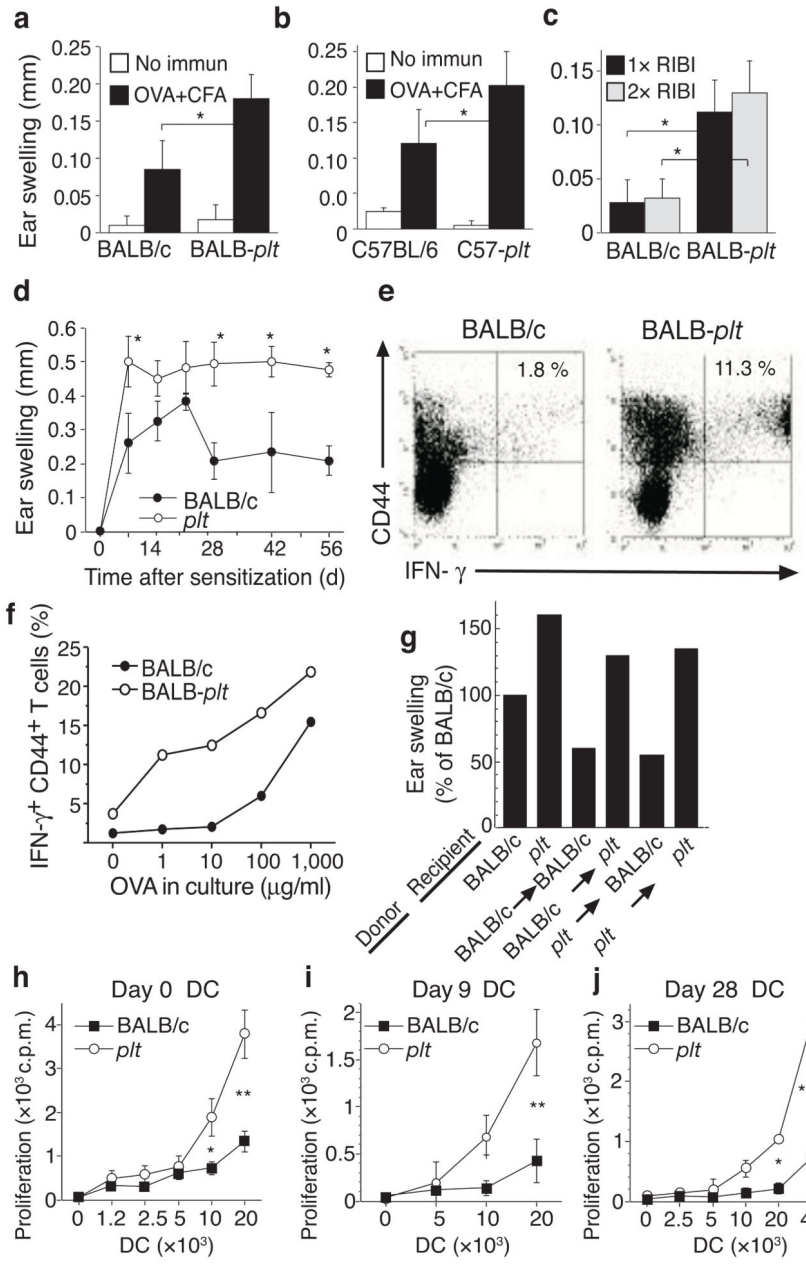

Figure 1.

Increased immune responses in *plt* mice. **(a–c)** DTH responses in *plt* mice. WT and *plt* mice were sensitized with OVA/CFA (**a,b**) or OVA/RIBI x1 or x2 (**c**). Responses were elicited after 7 days and ear swelling measured at 24 h. **(d)** Time course of contact hypersensitivity (CHS) responses. BALB/c and *plt* mice were sensitized by oxazolone skin painting and ear swelling measured 24 h after elicitation. Data points represent mean ± SD for 5 mice (**a–d**). **(e)** IFN-γ intracellular staining of BALB/c and *plt* lymph node $CD4^+$ T cells 9 days after immunization with OVA/CFA. Numbers indicate percentage of $CD44^+IFN\text{-}\gamma^+$ cells among $CD4^+$ T cells. **(f)** Percentage of $CD44^+IFN\text{-}\gamma^+$ cells among $CD4^+$ T cells after restimulation with increasing concentrations of OVA. **(g)** DTH responses, performed as above, after

reciprocal bone marrow transplantation between BALB/c and BALB/c-*plt* mice. Bars represent mean ear swelling as a percentage of the responses in BALB/c mice. n = 5 mice/group, P<0.02 for BALB/c vs. *plt* recipients. **(h)** Allogeneic T cell proliferation induced by lymph node $CD11c^+$ cells from untreated mice. **(i,j)** OVA-specific proliferation of a DO11.10 CD4 T cell line induced by total lymph node DCs 9 days (i) or 28 days (j) after immunization with OVA/CFA. Points represent mean ± SD for 3 mice (h j). * $P < 0.05$; ** $P < 0.005$; *** $P < 0.0005$ by Student's t-test.

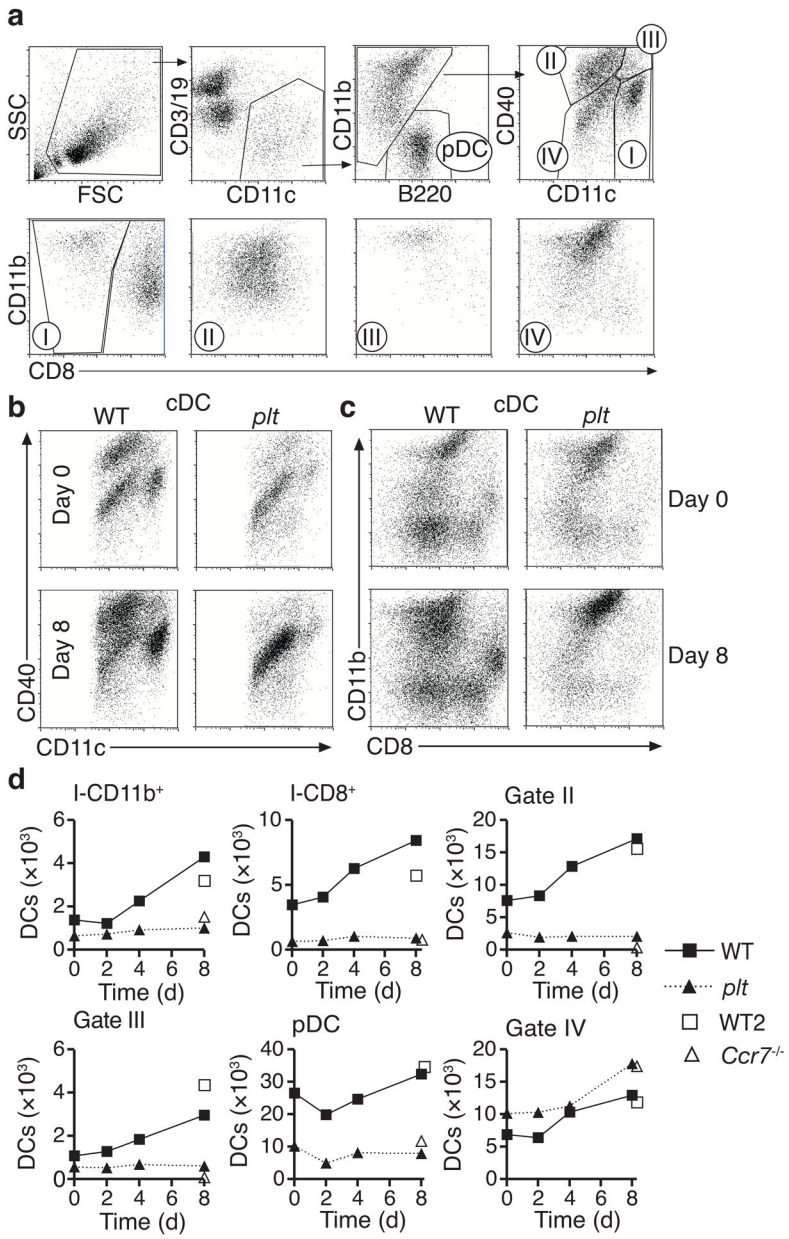

Figure 2.

Quantification of individual lymph node DC subtypes in BALB/c and *plt* mice. **(a)** Gating protocol for identification of lymph node DC subsets. Subtypes indicated include $CD11b^{-}$ $B220^{+}$ plasmacytoid DCs (pDC), $CD11c^{hi}CD40^{int}$ DCs (I), $CD11c^{int}CD40^{hi}$ dermal DCs (II), $CD11c^{hi}CD40^{hi}$ Langerhans-derived DCs (III), and $CD11c^{int}CD40^{int}$ inflammatory DCs (IV). DCs in gate I are further divided into $CD11b^{hi}CD8^{-}$ and $CD8^{+}$ DCs. **(b)** CD40 vs. CD11c, and (**c**) CD11b vs. CD8 flow profiles of BALB/c and *plt* lymph node $CD11c^{+}CD11b^{+}B220^{-}$ DCs (cDC) at baseline and 8 days after immunization with OVA/CFA. **(d)** Quantification of individual DC types in BALB/c, *plt*, and $Ccr7^{-/-}$ draining lymph nodes on the indicated days after footpad immunization with 20 μg OVA/CFA based on the

gates shown in (**a**). Points represent the cell number per lymph node in samples pooled from 3 mice. Data is representative of 3 separate studies.

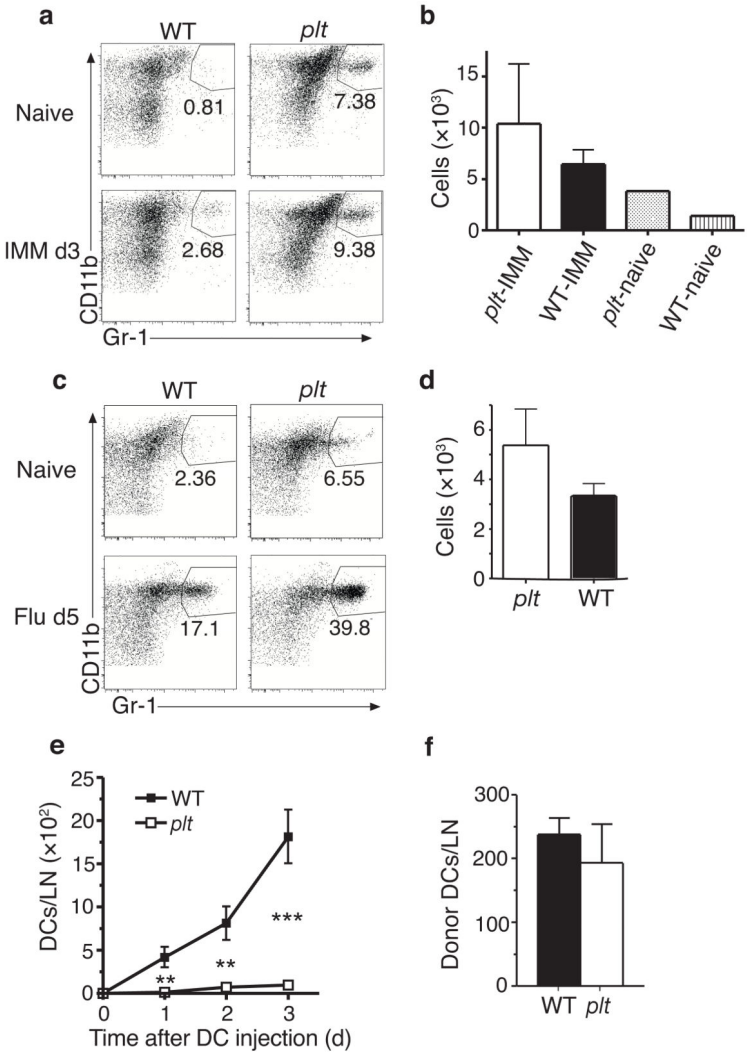

Figure 3.

Accumulation of inflammatory DCs in the draining lymph nodes of *plt* and WT mice. **(a,b)** $CD11b^{hi}Gr\text{-}1^{+}$ DCs in BALB/c and *plt* lymph nodes at baseline and 3 days after immunization with 100 μg OVA/CFA. (**a**) CD11b vs. Gr-1 flow profiles of $CD11c^{+}CD11b^{+}B220^{-}CD8^{-}$ lymph node cells. (**b**) Mean number ± SD of $CD11b^{hi}Gr\text{-}1^{+}$ DCs per 4 lymph nodes 3 days after immunization. $n = 3$ mice, $P > 0.05$. **(c,d)** $CD11b^{hi}Gr\text{-}1^{+}$ DCs in BALB/c and *plt* mediastinal lymph nodes at baseline and 5 days after influenza infection. (**c**) CD11b vs. Gr-1 flow profiles as in (**a**). (**d**) Mean number ± SD of $CD11b^{hi}Gr\text{-}1^{+}$ DCs per mediastinal lymph node. $n = 3$ mice, $P > 0.05$. **(e)** Time course of donor BM-derived DC accumulation in the popliteal lymph nodes of WT and *plt* mice. DCs were injected into footpads 3 days after injection of CFA. $n = 3$–4 mice. **(f)** Accumulation of donor moDCs ($CD45.1^{+}CD11c^{+}CD11b^{+}CD86^{+}$) in the draining lymph nodes of wild-type and *plt* mice 3 days after monocyte transfer. Monocytes were injected by tail vein 3 days after immunization of OVA/CFA. $n = 3$ mice, $^{*}P < 0.05$; $^{**}P < 0.005$; $^{***}P < 0.0005$ by Student's *t*-test.

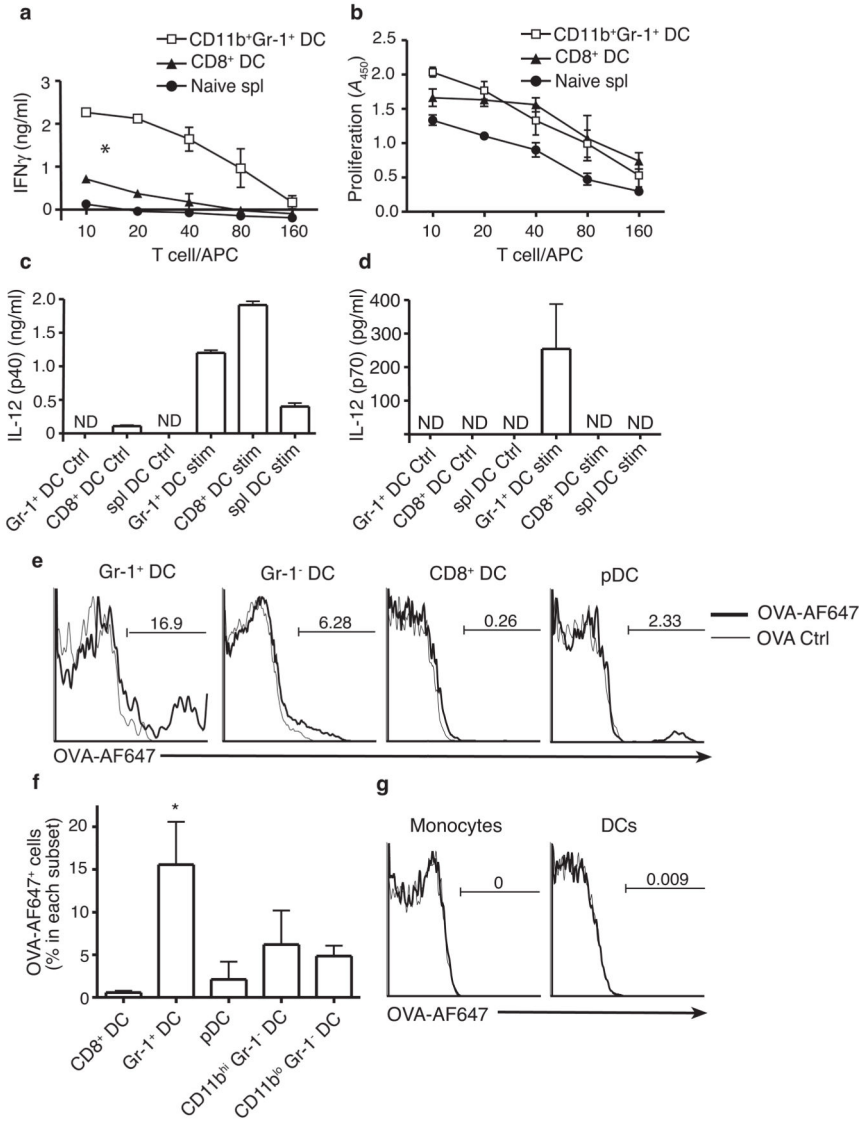

Figure 4.

Activities of CD11b^{hi}Gr-1$^+$ DCs. (**a,b**) CD8$^+$ DCs and CD11b^{hi}Gr-1$^+$ DCs, purified from the mediastinal lymph nodes of C57BL/6 mice 4 days after influenza infection, and total naive splenic DC were used to stimulate naive OT2 CD4$^+$ T cells in the presence of OVA peptide. Significant differences in slopes of response curves were calculated by ANOVA. *p<0.01 for Gr-1$^+$ DC vs. all other DC types. **(a)** IFN-γ production by stimulated OT2 cells as measured by ELISA. (**b**) Proliferation of stimulated OT2 cells as measured by BrdU incorporation in a colorimetric assay. **(c,d)** IL-12 production by DC subtypes. 2 × 10^4 CD8$^+$, CD11b^{hi}Gr-1$^+$, or splenic DCs were purified as above and cultured in media alone (Ctrl) or with LPS and αCD40 (Stim). After 24 h, IL-12p40 (**c**) and IL-12p70 (**d**) concentrations in the supernatants were measured by ELISA. (**a**–**d**) All data points indicate mean ± SD for 3 experiments, each using cells pooled from 5 to 7 mice. (**e**–**g**) Wild-type mice were immunized with OVA+CFA or OVA-AF647+CFA in the back. Brachial lymph nodes and blood were harvested 3 days later for flow analysis. *n* = 3 mice. (**e**) Flow histogram of OVA-

AF647 for each lymph node DC subset. (**f**) Mean percentage of OVA-AF647$^+$ cells in each DC subset. * $P < 0.05$ vs. all other DC types by ANOVA. (**g**) Histogram of OVA-AF647 accumulation in blood monocytes and DCs.

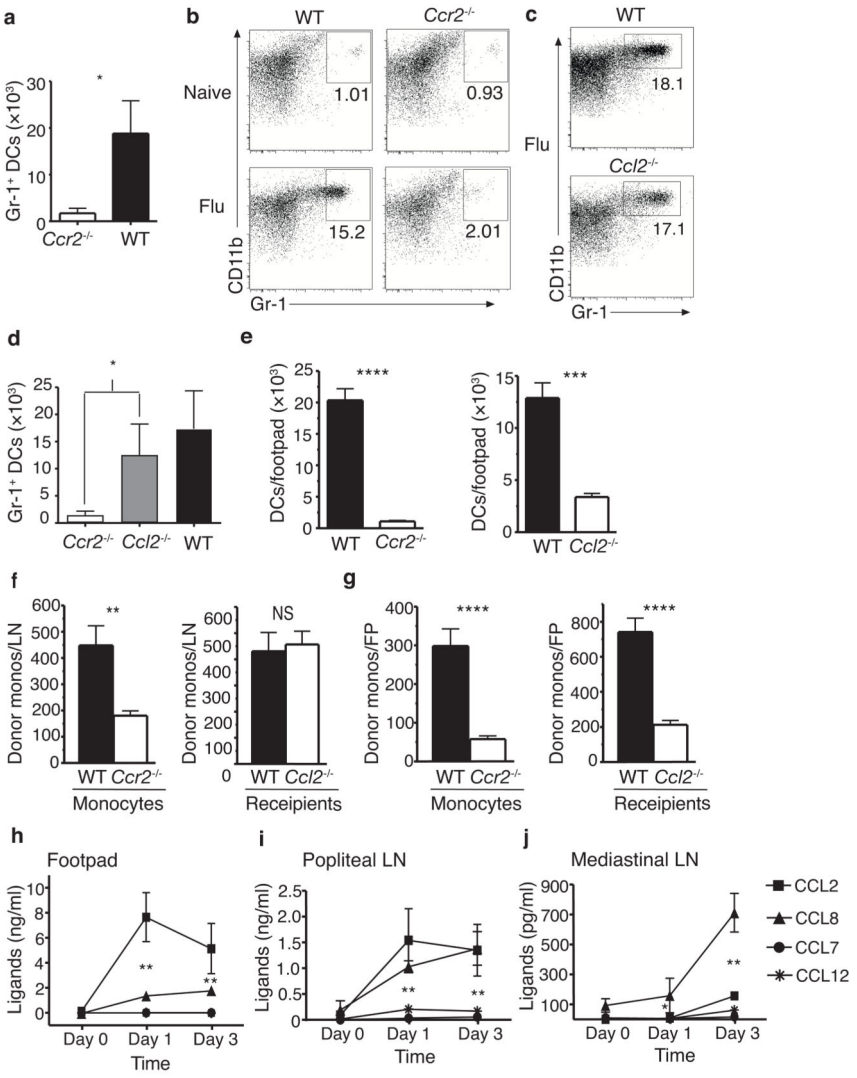

Figure 5.

Chemokine dependence of inflammatory DC accumulation. **(a)** Number of CD11b^{hi}Gr-1^{+} DCs per 4 draining lymph nodes in *Ccr2*$^{-/-}$ and C57BL/6 (WT) mice 3 d after immunization with OVA/CFA. Significance determined by Student's *t*-test, *n* = 3 mice. **(b,c)** Flow profiles of CD11c^{+}CD11b^{+}B220^{-} CD8^{-} mediastinal lymph node cells in WT and *Ccr2*$^{-/-}$ mice **(b)**, or WT and *Ccl2*$^{-/-}$ mice **(c)** at baseline and 5 d after influenza infection. **(d)** Number of CD11b^{hi}Gr-1^{+} DCs per lymph node in mice described in (**b,c**). Significance determined by ANOVA using Bonferroni's multiple comparison test. *n* = 6 mice. (**e**) Accumulation of CD11c^{+}CD11b^{+} DCs in footpads of WT, *Ccl2*$^{-/-}$ and *Ccr2*$^{-/-}$ mice 3 d post OVA/CFA injection. *n* = 10. **(f,g)** Number of donor monocytes in inflamed draining lymph nodes (**f**) and footpads (g) 2 h after i.v. injection. *n* = 10. Left: mean ± SD of WT or *Ccr2*$^{-/-}$ CD11b^{+}Ly6C^{hi}CD45.2^{+} donor cells per WT recipient (CD45.1) lymph node or FP. Right: mean ± SD of WT CD11b^{+}Ly6C^{hi} donor cells per WT or *Ccl2*$^{-/-}$ recipient lymph node or FP. Significance determined by Student's *t*-test. **(h–j)** Concentration of CCR2 ligands in footpads (**e**), and popliteal lymph nodes (**f**) after footpad injection of OVA/CFA, and in

mediastinal lymph nodes (**g**) after influenza infection, as determined by ELISA. $n = 3–4$ mice. Significance determined by ANOVA for CCL2 vs. CCL8 (**h,j**) or both CCL2 and CCL8 vs. CCL7 and CCL12. *$P < 0.05$; ** $P < 0.005$; *** $P < 0.0005$; **** $P < 0.00005$

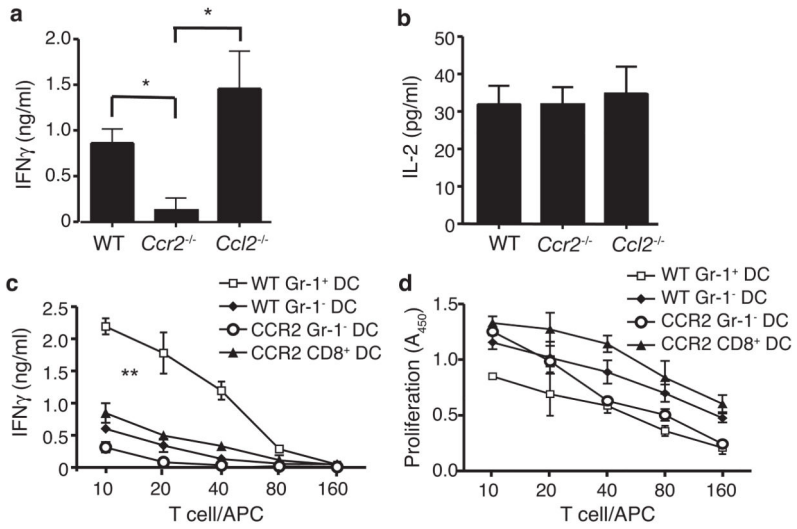

Figure 6.

T_H1 responses in the lymph nodes of *Ccr2*$^{-/-}$ and *Ccl2*$^{-/-}$ mice. (**a**–**b)** IFN-γ (a) and IL-2 (**b**) production by total lymph nodes cells isolated from WT, *Ccr2*$^{-/-}$ and *Ccl2*$^{-/-}$ mice 6 days after immunization with OVA/CFA. T cells were restimulated with OVA for 48 h and IFN-γ in the supernatant measured by ELISA. Data points represent mean ± SD, $n = 3$ mice. Significance determined by Student's *t*-test. *p<0.05 (**c,d**) IFN-γ production by (**c**) and proliferation of (**d**) OT2 cells stimulated as in Fig. 4a with the indicated DC types. Data points represent mean ± SD for 3 experiments, each using cells pooled from 5–7 mice. Response curves were analyzed by linear regression, and *P*-value for slopes was determined by ANOVA. **p<0.0001 for WT Gr-1$^+$ DC vs. all other DC types.